Carcinogenesis, 2015, Vol. 36, No. 4, 487–497

doi:10.1093/carcin/bgv012
Advance Access publication March 4, 2015
Original Manuscript

ORIGINAL MANUSCRIPT

Conditional disruption of *rictor* demonstrates a direct requirement for mTORC2 in skin tumor development and continued growth of established tumors

Theresa D.Carr[1], Robert P.Feehan[1], Michael N.Hall[2], Markus A.Rüegg[2] and Lisa M.Shantz[1,*]

[1]Department of Cellular and Molecular Physiology, The Pennsylvania State University College of Medicine, Hershey, PA 17033, USA and [2]Biozentrum, University of Basel, CH-4056 Basel, Switzerland

*To whom correspondence should be addressed. Tel: +1 717 531 1562; Fax +1 717 531 7667;Email: lms17@psu.edu

Abstract

Activation of signaling dependent on the mammalian target of rapamycin (mTOR) has been demonstrated in a variety of human malignancies, and our previous work suggests that mTOR complex (mTORC) 1 and mTORC2 may play unique roles in skin tumorigenesis. The purpose of these studies was to investigate the function of mTORC2-dependent pathways in skin tumor development and the maintenance of established tumors. Using mice that allow spatial and temporal control of mTORC2 in epidermis by conditional knockout of its essential component Rictor, we studied the effect of mTORC2 loss on both epidermal proliferation and chemical carcinogenesis. The results demonstrate that mTORC2 is dispensable for both normal epidermal proliferation and the hyperproliferative response to treatment with tetradecanoyl phorbol acetate (TPA). In contrast, deletion of epidermal Rictor prior to initiation in DMBA/TPA chemical carcinogenesis was sufficient to dramatically delay tumor development and resulted in reduced tumor number and size compared with control groups. Silencing of Rictor expression in tumor-bearing animals triggered regression of established tumors and increased caspase-3 cleavage without changes in proliferation. *In vitro* experiments demonstrate an increased sensitivity to caspase-dependent apoptosis in the absence of *rictor*, which is dependent on mTORC2 signaling. These studies demonstrate that mTORC2 activation is essential for keratinocyte survival, and suggest that inhibition of mTORC2 has value in chemoprevention by eliminating carcinogen-damaged cells during the early stages of tumorigenesis, and in therapy of existing tumors by restricting critical pro-survival pathways.

Introduction

The mammalian (mechanistic) target of rapamycin (mTOR), a central regulator of cell growth that is activated by a number of cancer-promoting mutations in upstream signaling pathways, exists in at least two distinct multi-protein complexes. Association of mTOR kinase with Raptor defines mTOR complex 1 (mTORC1), whereas Raptor is replaced by Rictor and mSIN1 in mTORC2. Activation of mTORC1 controls protein synthesis and ribosome biogenesis by phosphorylating the key regulators 4EBP1 and p70S6K1 (1). Although the function of mTORC2 is less understood, it has been shown to phosphorylate several AGC kinases. The best studied of these is Akt (protein kinase B), which promotes cell survival and proliferation when phosphorylated by mTORC2 at the hydrophobic motif site Ser-473 (2,3). mTORC2 has also been implicated in control of actin cytoskeletal organization at least in part by phosphorylation of another group of AGC kinases, the conventional protein kinase C isotypes (cPKCs) (4–6). Control of F-actin formation in fibroblasts was the first characterized function of mTORC2 (4,7). More recent studies in cancer cell lines have suggested that mTORC2 signaling alters actin cytoskeletal organization and cell motility in tumor invasion (8–11).

Because of their central location in cell metabolism, both mTOR complexes are potentially of great importance in

Received: October 13, 2014; **Revised:** January 26, 2015; **Accepted:** February 15, 2015

Abbreviations

4OHT	4-hydroxytamoxifen
BrdU	5-bromo-2-deoxyuridine
CC3	Cleaved caspase-3
DMBA	7,12-dimethyl-benz[a]anthracene
DMSO	dimethyl sulfoxide
FoxO	forkhead box
H&E	hematoxylin and eosin
i.p.	intraperitoneal
iRicKO	inducible rictor knockout
MEF	mouse embryo fibrobasts
mTOR	mammalian target of rapamycin
mTORC	mTOR complex
PBS	phosphate-buffered saline
PKC	protein kinase C
TPA	12-O-tetradecanoylphorbol-13-acetate
UVB	Ultraviolet B

oncogenic transformation. The selective mTORC1 inhibitor rapamycin and its analogues are currently in clinical trials or have been approved as therapy against several malignancies. Although combination trials are more promising, the use of these agents as monotherapy has had limited success (12). This may be explained by several key findings. First, amplified Akt signaling has been documented in the presence of rapamycin, due to relief of a p70S6K1-dependent feedback loop targeting PI3-kinase (4,7,13,14). Loss of this feedback inhibition in some, though not all, cancer cells may have the effect of enhancing cell survival with rapamycin treatment. Also of significance was the observation that the initiation and progression of prostate cancer induced by loss of the tumor suppressor PTEN, which results in hyperactivation of Akt, was more effectively suppressed by conditional deletion of mTOR than by rapamycin treatment (15). This result was due to continued activity of mTORC2 in the presence of rapamycin that is eliminated when mTOR is deleted, and suggested that the requirement for mTORC2 activity in prostate tumor development is related to the activation state of Akt. Since aberrant activation of Akt is a feature of many tumor types, the possibility that mTORC2 can directly drive tumorigenesis through this pathway must be considered. In support of this concept, studies have shown that the majority of gliomas contain high levels of *p*-Akt^{S473}, and both activity of mTORC2 and levels of Rictor were elevated in primary cells from gliomas compared with cells derived from normal surrounding brain tissue (8). Other work suggests that Rictor confers cisplatin resistance to ovarian cancer cells by activating Akt (16). In the skin, mTORC2 signaling is upregulated in human squamous cell carcinoma (17,18), and sustained Akt activation and increased Rictor have been demonstrated in mouse models of non-melanoma skin cancer (19–22). These findings led us to investigate whether skin tumorigenesis requires mTORC2-dependent signaling.

The most widely used models for the study of epithelial skin tumor development are the mouse models of initiation and promotion. Initiation is caused by a carcinogen-induced genetic change in epidermal stem cells. This can be accomplished by the topical application of 7,12-dimethyl-benz[a]anthracene (DMBA), which produces a signature mutation in codon 61 of the c-Ha-*ras* gene. Tumor promotion is stimulated by multiple applications of an agent such as the phorbol ester 12-O-tatradecanoylphorbol-13-acetate (TPA), which stimulates epidermal cell proliferation and hyperplasia (23). During promotion, initiated cells undergo clonal expansion, resulting in premalignant papillomas. The progression of papillomas to squamous cell carcinomas is strain-dependent and occurs stochastically; there is an increased probability of additional genetic alterations as the cell population expands. This model has been used extensively to study the effects of a variety of drug treatments and genetic manipulations on tumor formation and regression, including recent studies demonstrating that rapamycin potently inhibits tumor promotion (24).

Our previous results suggest that mTORC2 plays a critical role in pro-survival/anti-apoptotic signaling in keratinocytes following exposure to the complete carcinogen ultraviolet B (UVB) irradiation (25). We therefore hypothesized that mTORC2-induced activation of pro-survival signaling contributes to skin tumorigenesis. Here we use mouse models with stage-specific deletion of Rictor in the basal layer of the epidermis to extend our previous findings, and establish an essential role for mTORC2-controlled pathways in both skin tumor development and maintenance.

Materials and methods

Generation of K14-CreER^{T};Rictor$^{L/L}$ mice

Floxed Rictor mice (Rictor$^{L/L}$) contain LoxP sites flanking exons 4 and 5 of the *rictor* gene (26,27) (Figure 1A). These mice were crossed with K14-CreER^{T} mice (28) expressing a tamoxifen-activated Cre recombinase fused to a modified estrogen receptor under control of the Keratin 14 promoter (Jackson Labs, Bar Harbor, ME). Cre induces recombination in the outer root sheath of the hair follicle and the epidermal basal layer upon treatment with 4-hydroxytamoxifen (4OHT; Sigma, St. Louis, MO). K14-CreER^{T} mice were bred with Rictor$^{L/L}$ mice to generate K14-CreER^{T};Rictor$^{L/L}$ mice (Cre-Rictor$^{L/L}$ mice), which are hemizygous for the K14-CreER^{T} transgene and homozygous for the floxed *rictor* allele. Tail DNA was isolated using REDExtract-N-Amp PCR Kit (Sigma). All animals were backcrossed for 10 generations onto the C57BL/6 background. Experiments involving mice were carried out in compliance with the Guide for the Care and Use of Laboratory Animals and protocols were approved by the Animal Care and Use Committee of the Pennsylvania State University College of Medicine.

Cell culture

Primary keratinocytes were isolated from 1- to 3-day old pups as described previously (25). Cell suspensions were plated at a density of one-half mouse equivalent per 60 mm^2 plate, and the medium was changed every other day. Cultures were supplemented with 2 nM 4OHT (Sigma) [1:1000 in dimethyl sulfoxide (DMSO)] for 4 days to induce recombination.

Mouse embryo fibrobasts (MEFs) with constitutive deletion of *rictor* (Rictor$^{Ex3del/Ex3del}$) and wild-type controls (Rictor$^{Ex3cond/wt}$), abbreviated Rictor$^{-/-}$ and Rictor$^{+/+}$ (a generous gift from Dr Mark Magnuson, Vanderbilt University, Nashville, TN), were grown as described previously (25). MEFs with inducible *rictor* knockout (iRicKO cells) were isolated from Rictor$^{L/L}$ mice, infected with a retrovirus carrying a tamoxifen-inducible Cre recombinase (CreER^{T2}), and selected for stable integration of the virus (29). Deletion of the floxed *rictor* allele was induced by addition of 2 nM 4OHT to the culture medium daily for 3 days, and cells were exposed to UVB on day four. Experiments were performed when cells reached 70–80% confluence. Cell lines were used at passage <20 and were authenticated through verification of the wild-type or floxed *rictor* allele, cell morphology monitoring and growth curve analysis. Cells undergo routine mycoplasma contamination checks and were last checked in August, 2013.

Stage-specific disruption of rictor signaling during two-stage carcinogenesis

Three groups of mice (control groups = Cre-Rictor$^{L/L}$ + vehicle and Rictor$^{L/L}$ + 4OHT; experimental group = Cre-Rictor$^{L/L}$ + 4OHT) were used at 6–8 weeks of age. The dorsal surface was shaved and mice were allowed to rest for 24–48 h. Only mice in telogen (resting phase of the hair cycle) were used for experiments. Animals were treated topically with 2 mg 4OHT in 100 µl or vehicle (DMSO:Acetone [1:9]) daily for five consecutive days. Three days after the final 4OHT treatment, mice were initiated with a single topical dose of DMBA (400 nmol; Kodak Laboratory Chemicals, Rochester, NY) in 200 µl acetone. One week after initiation, mice began treatment with

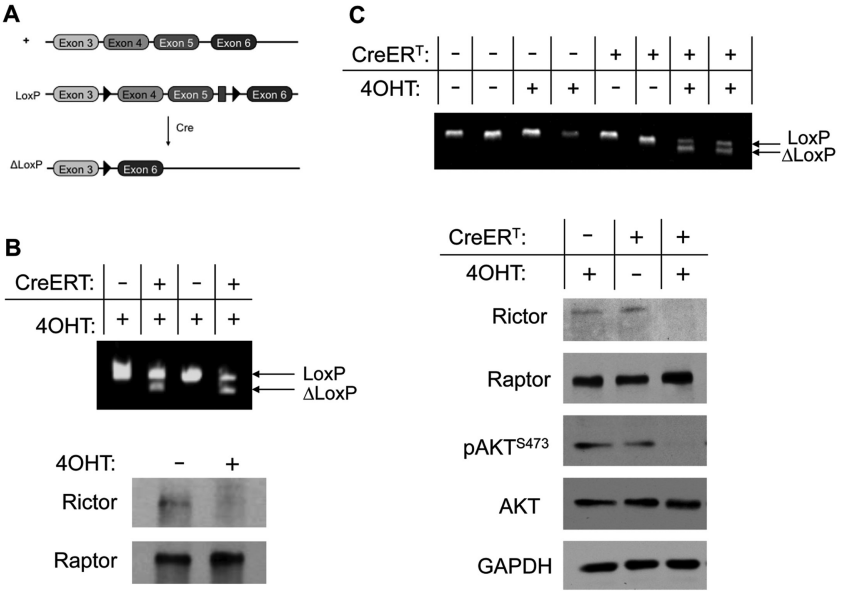

Figure 1. 4OHT induces LoxP recombination and Rictor deletion in epidermis and primary keratinocytes of Cre-Rictor$^{L/L}$ mice. (**A**) Schematic representation of the *rictor* allele targeted for K14-Cre-mediated recombination. (**B**) 7-week old Cre-Rictor$^{L/L}$ mice were treated topically with 2-mg 4OHT or vehicle daily for 5 days. *Top*, PCR analysis of epidermal DNA harvested 7 days after final 4OHT treatment. ΔLoxP denotes primers specific to the recombined *rictor* allele. *Bottom*, immunoblot analysis of Raptor and Rictor in epidermal extracts harvested 7 days after final 4OHT treatment. Data are representative of two experiments. (**C**) Cre-Rictor$^{L/L}$ and Rictor$^{L/L}$ keratinocytes were harvested from 1–3 day-old pups and cultured in 4OHT (2 nM) or vehicle for 3 days. *Top*, PCR analysis of primary keratinocyte DNA harvested 24 h after final 4OHT treatment. ΔLoxP denotes primers specific to the recombined Rictor allele. *Bottom*, immunoblot analysis of Rictor in primary keratinocyte whole-cell lysates. Data are representative of 2–3 independent experiments.

topical TPA (17 nmol) in 200 µl acetone twice weekly for 21 weeks. Mice were monitored weekly for tumor formation, and the dimensions of skin tumors greater than 1 mm × 1 mm were recorded. Surface area was calculated as (length × width).

To analyze the effect of *rictor* deletion on continued growth of existing papillomas, Cre-Rictor$^{L/L}$ and Rictor$^{L/L}$ mice were subjected to two-stage skin carcinogenesis as described above to generate papillomas. Animals that developed tumors of at least 3 mm × 2 mm were treated with 2 mg of 4OHT (in 100 µl DMSO:sunflowerseed oil [1:9]) intraperitoneal (i.p.) for five consecutive days and this regimen was repeated every 2 weeks. The change in tumor dimensions was monitored weekly for 4 weeks. All mice continued to receive TPA treatment twice weekly for the remainder of the experiment.

Short-term TPA experiments

After treatment of 6- to 8-week old mice with 4OHT or vehicle for 5 days, 17 nmol of TPA (Calbiochem-Novabiochem Corp., La Jolla, CA) in 200 µl of acetone was applied topically. For multiple TPA applications, mice were treated twice weekly for 2 weeks at 3- to 4-day interval. Mice were euthanized by CO_2 asphyxiation at the indicated times, and skin was fixed in 10% neutral buffered formalin.

Histology and immunohistochemistry

For short-term TPA experiments, tissue sections were collected from mice 48 h after the final TPA treatment. Epidermal thickness was measured in hematoxylin and eosin (H&E) sections at five non-overlapping locations for each mouse. To assess epidermal proliferation, mice received i.p. injections of 100 mg/kg 5-bromo-2-deoxyuridine (BrdU; Sigma) in saline 1 h prior to euthanasia. Sections were stained with an anti-BrdU antibody as described previously (25). Epidermal labeling index was determined by calculating the percentage of cells positive for BrdU. At least 100 continuous basal cells were counted for each mouse at a minimum of three different non-overlapping locations. Apoptosis was assessed in tumors using immunohistochemical staining with cleaved caspase-3 (CC3) antibody (Cell Signaling Technology, Beverly, MA) using 3–4 mice for each condition.

UVB treatment of cells in culture

Cells were washed twice with phosphate-buffered saline (PBS), then in a minimal volume of PBS exposed to UVB (FS20 UVB bulbs, National Biological, Cleveland, OH) at doses indicated. Bulb intensity was measured using a UVB 500C meter (National Biological). After irradiation, PBS was removed and conditioned medium with drug treatments was added back. Mock-irradiated cells were treated identically, but without UVB exposure. Torin-2 (Tocris Bioscience, Minneapolis, MN), rapamycin (Developmental Therapeutics Program, National Cancer Institute, Bethesda, MD) or DMSO were added to the culture medium at a 1:1000 dilution 1 h prior to UVB. Cell viability was determined colorimetrically by MTS assay (CellTiter 96 Aqueous Proliferation Assay, Promega, Madison, WI). Each condition was plated in triplicate and the experiments were repeated at least three times. Cell viability was calculated by setting the mean vehicle-treated mock UVB viability to 100%. Relative change in viability was calculated taking the ratio of cell viability of UVB to mock for each drug regimen. Where indicated, cells were preincubated with 50 µM Z-VAD-fmk (Cayman Chemical Co., Ann Arbor, MI) for 1 h prior to UVB to prevent caspase-dependent cell death.

Western blotting analysis

Cre-Rictor$^{L/L}$ and Rictor$^{L/L}$ mice were treated topically with 1 mg 4OHT in 100 µl or vehicle daily for five consecutive days. Animals were euthanized 14 days after the final treatment. Skin was treated with a depilatory agent, washed, excised and underlying fat and connective tissue were removed. Epidermal samples were collected by scraping the surface of excised skin with a razor blade and placed into ice-cold RIPA buffer (Santa Cruz Biotechnology, Santa Cruz, CA). Samples were sonicated, centrifuged and supernatants collected. Protein concentrations were determined using the Bio-Rad reagent (Bio-Rad). Equal amounts of protein were subjected to electrophoresis. For *in vitro* studies, cells were washed twice with ice-cold PBS and harvested directly into sodium dodecyl sulfate sample buffer, then boiled for 2 min and stored at –20°C until use. Western blotting was performed as described previously (25). Antibodies used include Rictor, Raptor, Akt, *p*-Akt^{Ser473}, *p*-Akt^{Thr308}, p70S6K, *p*-p70S6K^{Thr389}, PRAS40, *p*-PRAS40^{Thr246}, FoxO3a, *p*-FoxO1/3a$^{Thr24/Thr32}$, PKCα, *p*-PKCα/βII$^{Thr638/Thr641}$, Lamin B1, α-Tubulin (all from Cell Signaling Technology; 1:1000) and GAPDH (Proteintech, Chicago, IL; 1:2000).

Statistical analysis

The effect of Rictor deletion on tumor incidence was analyzed using log-rank analysis of Kaplan-Meier tumor-free survival curves. For tumor

multiplicity, differences in the average number of papillomas per mouse were analyzed using 2-way analysis of variance. Tumors were counted only if the length and width were both greater than 1 mm. Tumors in regression experiments were compared with their initial size using a two-tailed paired student's *t*-test. All other statistical comparisons utilized a two-tailed unpaired Student's *t*-test.

Results

Characterization of LoxP recombination and rictor deletion in Cre-Rictor$^{L/L}$ epidermis and primary keratinocytes

The early embryonic lethality caused by deletion of the *rictor* gene (30) led us to use a 4OHT-inducible Cre-LoxP system to selectively ablate *rictor* in mouse epidermal basal cells in order to investigate the role of mTORC2 in skin tumorigenesis. To validate the efficiency of *rictor* deletion in the epidermis of Cre-Rictor$^{L/L}$ mice, we used topical treatment of 4OHT or vehicle daily for 5 days. PCR analysis using DNA from the dorsal epidermis harvested from mice 1 week after the final 4OHT treatment verified that recombination occurred only in mice expressing the K14-CreER^{T} transgene and treated with 4OHT (Figure 1B). Immunoblot analysis of epidermal extracts confirmed reduced levels of Rictor in mice treated with 4OHT, but not vehicle-treated mice, and levels of Raptor were unchanged (Figure 1B). PCR and western blot analysis of primary keratinocytes isolated from Cre-Rictor$^{L/L}$ mice also verified recombination of the *rictor* allele (ΔLoxP) and *rictor* deletion in cells cultured with 4OHT, but not vehicle (Figure 1C). Western blots of Cre-Rictor$^{L/L}$ primary keratinocytes treated with 4OHT indicated Rictor and *p*-Akt^{Ser473} were below the limit of detection, whereas Raptor was unchanged (Figure 1C).

Measurement of normal keratinocyte proliferation in the presence of epidermal rictor deletion

To examine whether absence of epidermal Rictor results in defective keratinocyte proliferation, we analyzed the epidermis of Cre-Rictor$^{L/L}$ mice. H&E staining of paraffin-embedded sections showed that untreated epidermis was normal in structure of both follicular and interfollicular epidermis (Figure 2A). Application of 4OHT to induce recombination and *rictor* deletion caused no apparent change in morphology or in epidermal thickness (Figure 2A and B). When epidermal proliferation was analyzed by BrdU incorporation as a marker of DNA synthesis, labeling was almost absent in untreated epidermis, whereas topical application of 4OHT resulted in a moderate increase (Figure 2C and D). Although the reason for this increase is not known, no mice were found to develop skin abnormalities over

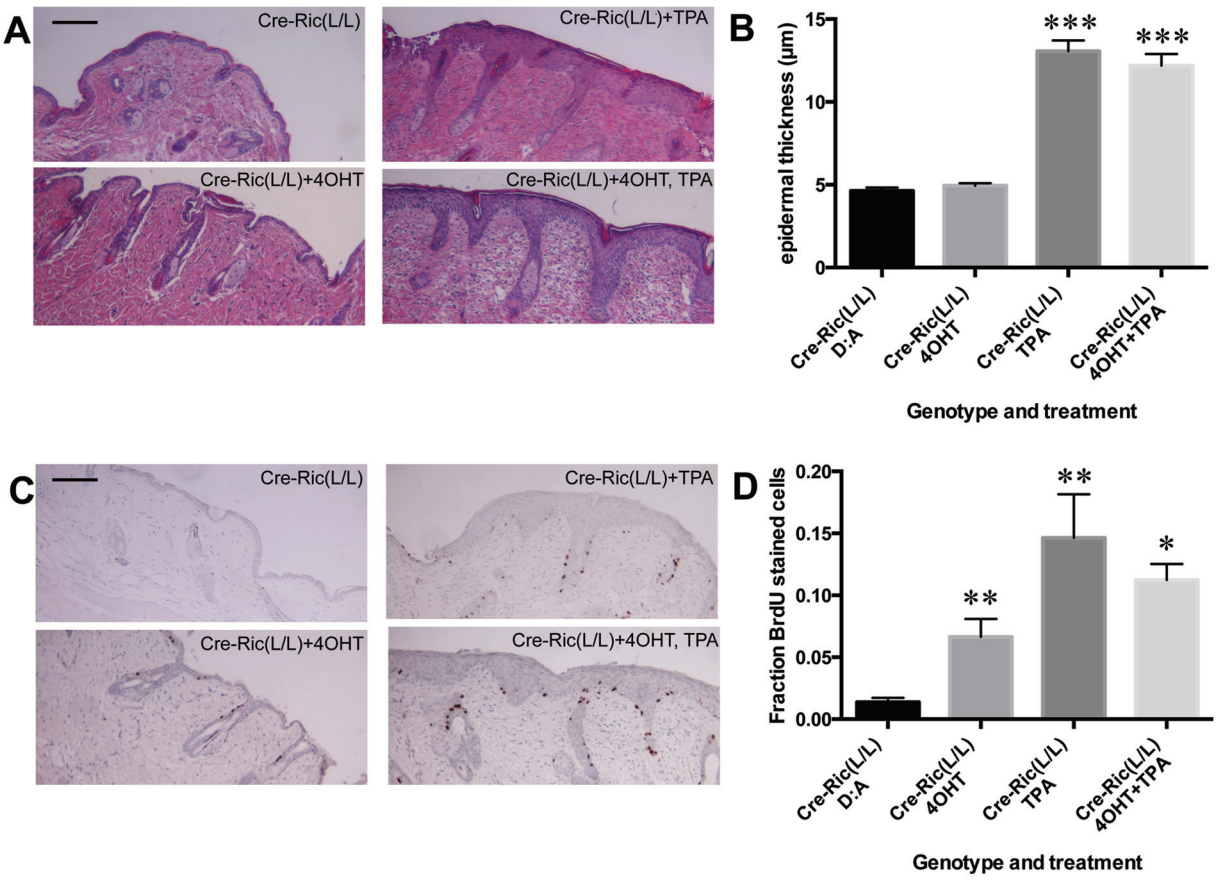

Figure. 2. Effect of *rictor* deletion on basal and TPA-stimulated epidermal proliferation. Cre-Rictor$^{L/L}$ mice at 7–8 weeks of age were treated topically with 4OHT (2 mg) or vehicle (D:A) daily for 5 days. A subset of mice from each group were then treated with either 17 nmol TPA or DMSO four times over a 2-week period. Mice were killed 6 h after the final TPA treatment. (**A**) Representative H&E images of skin sections (scale bar = 50 μm). (**B**) Quantitation of epidermal thickness (mean ± SEM) for $n = 4$ mice/group; ***$P < 0.0001$ for Cre-Rictor$^{L/L}$ TPA compared with Cre-Rictor$^{L/L}$ D:A; ***$P < 0.0001$ for Cre-Rictor$^{L/L}$ 4OHT+TPA compared with Cre-Rictor$^{L/L}$ 4OHT. (**C**) Representative BrdU incorporation of mice injected with 100 mg/kg BrdU 1 h before killing (scale bar = 50 μm). (**D**) Quantitation of BrdU labeling index (mean ± SEM) for $n = 4$ mice/group; **$P < 0.005$ for Cre-Rictor$^{L/L}$ 4OHT compared with Cre-Rictor$^{L/L}$ D:A; **$P < 0.005$ for Cre-Rictor$^{L/L}$ TPA compared with Cre-Rictor$^{L/L}$ D:A; *$P < 0.05$ for Cre-Rictor$^{L/L}$) 4OHT + TPA compared with Cre-Rictor$^{L/L}$ 4OHT. There is no statistical difference between Cre-Rictor$^{L/L}$ TPA and Cre-Rictor$^{L/L}$ 4OHT + TPA groups ($P = 0.3819$).

time following Rictor recombination, and mice have a normal life span (data not shown).

It has been shown previously that rapamycin has a dramatic inhibitory effect on TPA-induced epidermal hyperproliferation (24). Because prolonged exposure to rapamycin can also inhibit mTORC2 activity in some cancer models (31,32), we exposed mice with epidermal-specific *rictor* deletion to multiple applications of TPA to determine the role of mTORC2 in the TPA response. In contrast to the results reported with mTORC1 inhibition, loss of Rictor had no effect on epidermal hyperproliferation either by visual inspection (Figure 2A and C) or quantitative analysis (Figure 2B and D). Epidermal thickness of Cre-Rictor$^{L/L}$ mice treated with TPA alone was significantly greater than both vehicle- and 4OHT-treated mice, and the combination of 4OHT + TPA had no additional effect (Figure 2B). Similarly, BrdU incorporation was indistinguishable in mice treated with TPA alone compared with mice treated with 4OHT + TPA (Figure 2D). As mentioned above, addition of 4OHT alone increased the labeling index moderately compared with vehicle-treated mice, but epidermal BrdU incorporation in Cre-Rictor$^{L/L}$ mice + 4OHT was only about 50% of Cre-Rictor$^{L/L}$ mice treated with either TPA or with 4OHT + TPA (Figure 2D).

Rictor is necessary for skin tumorigenesis

To determine the role of Rictor during the initiation stage of skin carcinogenesis, mice were treated with 4OHT prior to initiation with a single topical dose of DMBA. One week later, mice were treated topically with TPA twice weekly for 21 weeks (Figure 3A). Using this protocol, we found that Cre-Rictor$^{L/L}$ mice are remarkably resistant to tumorigenesis. At the end of 21 weeks, there was a striking reduction in tumor incidence from 100% in both control groups to only 38% in the inducible Rictor-deficient mice ($P < 0.0001$, Figure 3B). In addition, Cre-Rictor$^{L/L}$ mice treated with 4OHT showed a delay in tumor development relative to the control groups, and the average number of papillomas per mouse was significantly lower from week nine until the end of the experiment ($P < 0.005$, Figure 3C). Rictor ablation in the basal epidermis also led to a dramatically lower tumor burden, with the average surface area of tumors in Cre-Rictor$^{L/L}$ mice + 4OHT reduced at least 90% compared with both control groups at the end of the experiment ($P < 0.005$, Figure 3D). Taken together with the results above, these data show that loss of Rictor in the basal cells of the epidermis attenuates tumor initiation without affecting proliferation of normal keratinocytes.

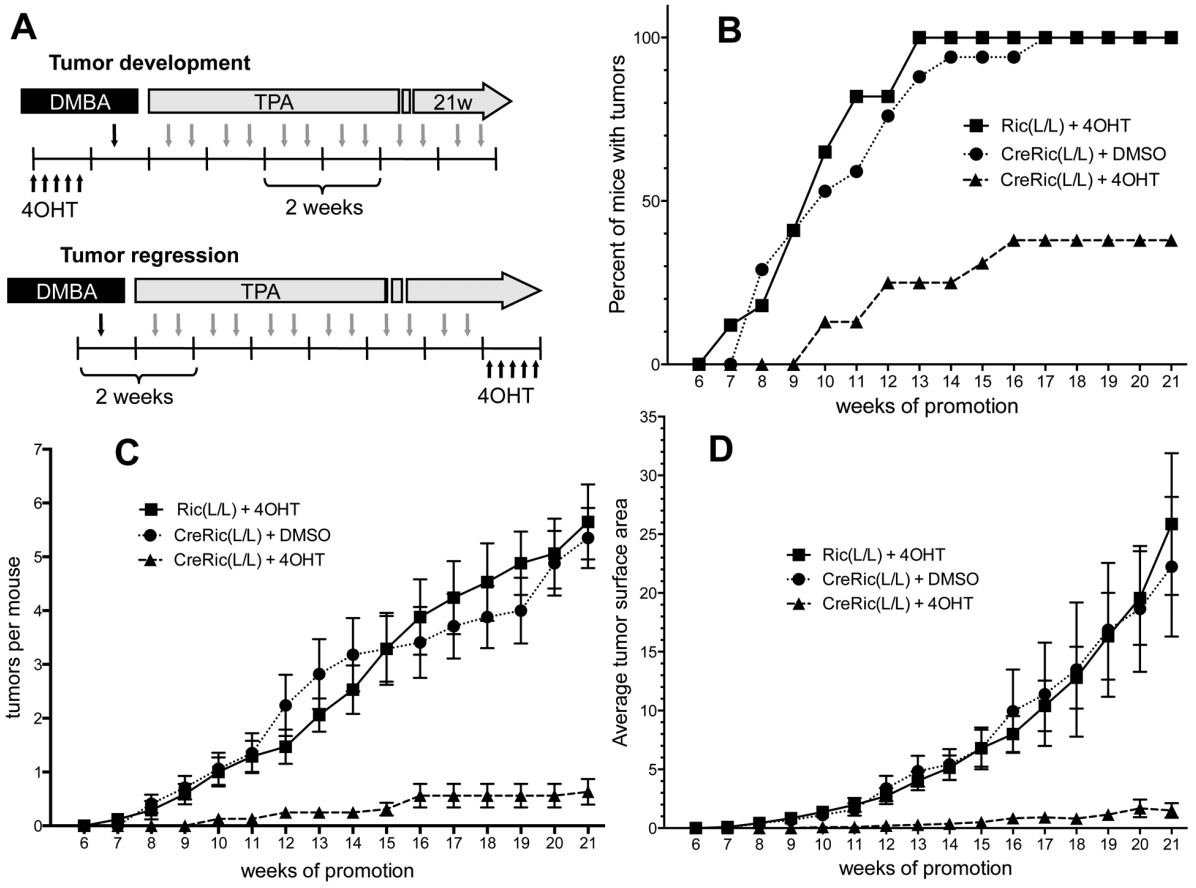

Figure 3. Effect of *rictor* deletion on two-stage skin carcinogenesis and tumor regression. Rictor-deficient mice [Cre-Rictor$^{L/L}$ + 4OHT $n = 16$] and two control groups [Cre-Rictor$^{L/L}$ + DMSO $n = 17$, Rictor$^{L/L}$ + 4OHT $n = 17$] were subjected to a two-stage skin carcinogenesis protocol. Papillomas greater than 1 mm × 1 mm were counted weekly. (**A**) Protocol used to examine the effect of *rictor* deletion on tumor development and maintenance. *Top,* for carcinogenesis experiments, *rictor* deletion was induced prior to 200 nmol DMBA initiation with topical application of 4OHT daily for five treatments. One week after DMBA initiation, mice received twice-weekly applications of 17 nmol TPA until the end of the experiment. *Bottom,* for tumor regression experiments, when tumors reached a minimum size of 3 mm × 2 mm, *rictor* deletion was induced with i.p. injections of 4OHT repeated daily for 5 days, and the regimen was repeated every 2 weeks. Twice weekly TPA treatments were continued and tumors were harvested 4 weeks after the initial 4OHT treatment. (**B–D**) Effect of *rictor* deletion prior to initiation on tumorigenesis. (**B**) Percentage of mice with papillomas. (**C**) Average number of tumors per mouse; mean ± SEM. (**D**) Average surface area of tumors per group; mean ± SEM.

Deletion of rictor in existing papillomas causes tumor regression

Previous results have demonstrated that treatment of tumor-bearing mice with rapamycin rapidly decreased tumor burden (24,33). To evaluate whether *rictor* deletion and mTORC2 inhibition in pre-existing papillomas blocked continued growth, a separate cohort of Cre-Rictor$^{L/L}$ and Rictor$^{L/L}$ mice were first subjected to two-stage skin carcinogenesis to generate papillomas, then treated with multiple i.p. injections of 4OHT over a 2-week period (Figure 3A). All mice continued to receive TPA treatment twice weekly for the remainder of the experiment. The results demonstrate that 4OHT-induced *rictor* disruption in tumors inhibited their further growth (Figure 4). Among the 12 tumors from Cre-Rictor$^{L/L}$ mice treated with 4OHT, 10 underwent a reduction in tumor size, whereas all tumors from identically-treated Rictor$^{L/L}$ mice either increased in size or remained constant (Figure 4A, Supplementary Table 1, available at *Carcinogenesis* Online). Additionally, the relative size of tumors in Cre-Rictor$^{L/L}$ mice was significantly smaller than in the control group ($P < 0.01$ at week four). Although the average tumor size in control mice increased significantly by the conclusion of the experiment ($P < 0.05$ relative to initial size), the surface area of tumors from inducible Rictor-deficient mice decreased significantly ($P < 0.05$) (Figure 4B). These results clearly indicate that inducible disruption of *rictor* in established tumors leads to their regression.

To determine the mechanism of tumor regression in response to *rictor* deletion, mice were killed 4 weeks after the beginning of the regression experiment (week 25 of the carcinogenesis experiment), and serial sections from paraffin-embedded tumors were analyzed. Examination of H&E sections from each genotype determined that all tumors (12 tumors from Cre-Rictor$^{L/L}$ mice and 8 tumors from Rictor$^{L/L}$ mice) were well-differentiated papillomas (Figure 4C). To establish whether loss of Rictor decreases tumor cell proliferation, mice were injected with BrdU and tumors were analyzed for S-phase cells. Although

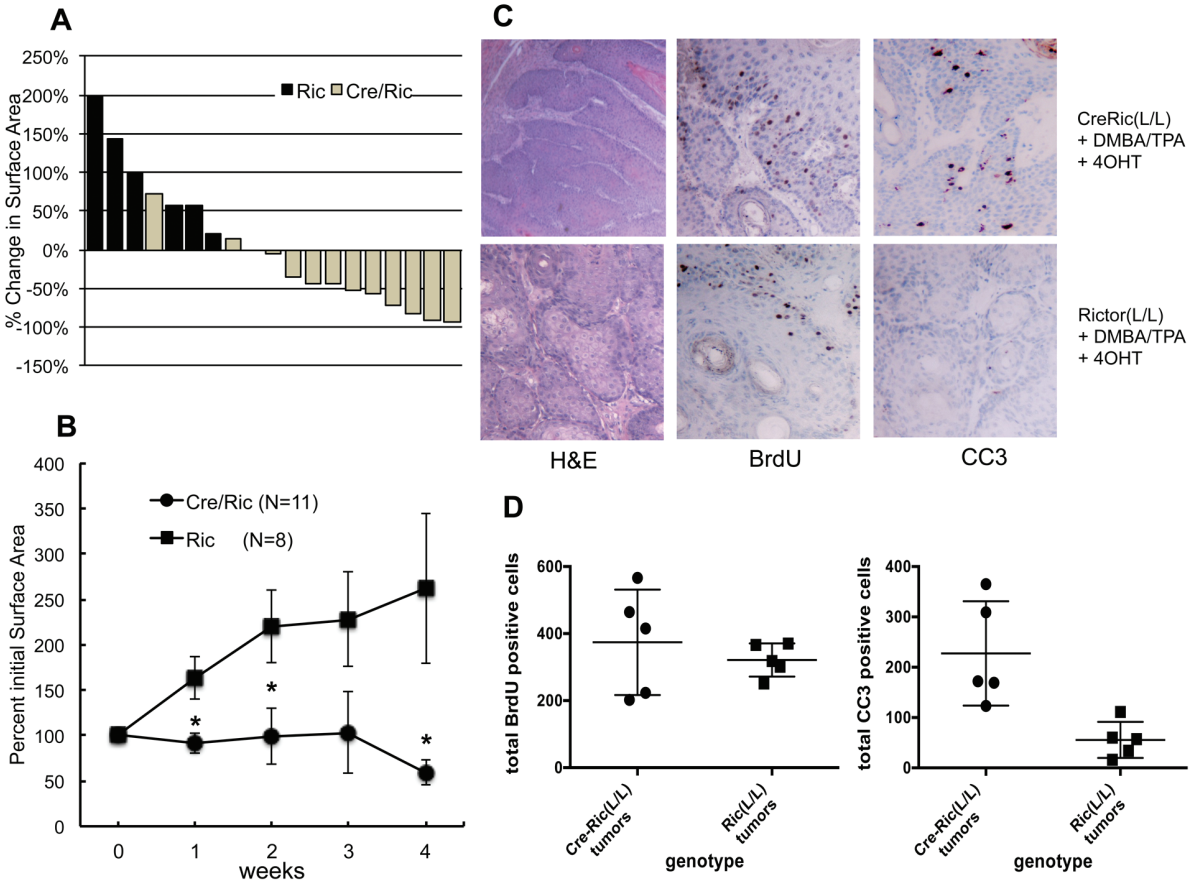

Figure 4. Effect of *rictor* deletion in established tumors. Cre-Rictor$^{L/L}$ and Rictor$^{L/L}$ mice were subjected to two-stage skin carcinogenesis as described in Figure 3 to generate papillomas. When tumor size reached at least 3 mm × 2 mm, mice were treated with 2 mg of 4OHT (in 100 µl DMSO:sunflowerseed oil [1:9]) i.p. for five consecutive days and this regimen was repeated every 2 weeks. Dimensions of tumors were measured prior to 4OHT treatment and weekly thereafter. Mice continued to receive TPA twice weekly. A total of 12 tumors were monitored in Cre-Rictor$^{L/L}$ mice (Cre/Ric; $n = 7$ mice), and 8 tumors were monitored in Rictor$^{L/L}$ mice (Ric; $n = 5$ mice). (**A**) Waterfall graph showing the percent change in surface area for each individual tumor relative to its initial size. One tumor from the Rictor$^{L/L}$ group did not change in surface area over the 4 weeks. One tumor from the Rictor$^{L/L}$ group increased in size by 700% and was not included. (**B**) Average percent change in surface area relative to initial size; mean ± SEM. * = significantly different from Rictor$^{L/L}$ mice ($P < 0.05$). (**C**) Histological analysis of tumors from Cre-Rictor$^{L/L}$ and Rictor$^{L/L}$ mice 4 weeks after 4OHT treatment. *Left*, typical keratinocyte-derived exophytic lesions of the skin in both experimental groups. *Middle*, mice were injected with BrdU (100 mg/kg, i.p.) 1 h before killing and proliferating cells were stained with an anti-BrdU antibody as described in the Materials and Methods. Results are representative of all tumors taken from 7 Cre-Rictor$^{L/L}$ and 5 Rictor$^{L/L}$ mice. *Right*, tumors were analyzed for expression of CC3 as described in the Materials and Methods. Results are representative of multiple tumors taken from 3–4 mice in each group. (**D**) Quantitation of BrdU and CC3 results in C. Total positive cells in four non-overlapping fields were counted for each tumor. Five tumors from each genotype were quantitated, and results are expressed as mean ± SEM, shown as line with error bars. CC3-positive cells are significantly different between the two groups, $P < 0.01$. BrdU incorporation was not different between the groups.

tumors from 4OHT-injected Cre-Rictor$^{L/L}$ mice were strikingly smaller than those from Rictor$^{L/L}$ mice treated in the same way (Figure 3D), tumors from both groups demonstrate similar incorporation of BrdU (Figure 4C and D). This is consistent with the unaltered hyperproliferation response observed in the skin of Rictor-deficient mice after TPA treatment (Figure 2). In contrast, regressing tumors from Cre-Rictor$^{L/L}$ mice show patches of strong staining for CC3 whereas significantly less CC3 staining is observed in tumors isolated from Rictor$^{L/L}$ mice (Figure 4C and D), suggesting that Rictor loss sensitizes tumors to apoptosis and subsequent regression even in the continued presence of a promoting stimulus.

Increased sensitivity to UVB-induced apoptosis upon *rictor* deletion *in vitro* is dependent on mTORC2

The results in Figure 4 are consistent with increased apoptosis in DMBA/TPA-induced tumors upon *rictor* ablation. We have also shown previously that Rictor$^{-/-}$ MEFs were sensitized to UVB-induced apoptosis (25). To directly address the question of whether increased cell death in the absence of Rictor is dependent on mTORC2, we used wild-type and *rictor*-null MEFs exposed to UVB and treated with either the TOR kinase inhibitor Torin-2 or the mTORC1 inhibitor rapamycin (Figure 5). We first tested the ability of rapamycin or Torin-2 to inhibit UVB-induced activation of mTOR signaling. Western blot analysis showed that in wild-type cells both Torin-2 and rapamycin completely blocked UVB-induced phosphorylation of p70S6K1^{T389}, a marker of mTORC1 activity. Torin-2 also reduced phosphorylation of Akt at the mTORC2 site S473, whereas rapamycin had no effect (Figure 5A). In Rictor$^{-/-}$ cells, both inhibitors prevented UVB activation of mTORC1 signaling, whereas Akt phosphorylation at Ser-473 was not measurable. Although Torin-2 increased UVB-mediated cell death in wild-type cells compared with treatment with either rapamycin or vehicle control, it did not have a similar effect in Rictor$^{-/-}$ cells (Figure 5B), suggesting that the increased cell death in Rictor$^{-/-}$ cells is dependent on mTORC2 signaling. Western blots indicated increased caspase-3 cleavage of wild-type cells exposed to Torin-2, but not of Rictor$^{-/-}$ cells (Figure 5C). In addition, pre-incubation with the pan-caspase inhibitor Z-VAD-fmk significantly suppressed UVB-induced cell death in iRicKO cells in which *rictor* deletion was induced by treatment with 4OHT (Figure 5D). Taken together, these results demonstrate that loss of Rictor sensitizes cells exposed to UVB *in vitro* to caspase-dependent apoptosis. We further elucidated the role of mTORC2 in genotoxic stress by exposing iRicKO cells with and without *rictor* deletion to cisplatin, then performing clonogenic assays. Like exposure to UVB, increased cisplatin-induced cytotoxicity is observed in the absence of Rictor (Supplementary Figure 1A and B is available at *Carcinogenesis* Online).

To further explore the potential biochemical mechanisms by which Rictor loss can sensitize cells to apoptosis, we examined activation of both mTORC1 and mTORC2 downstream effectors in iRicKO cells over a time course of 24 h post-UVB. UVB exposure led to a rapid, time-dependent phosphorylation of both p70S6K1^{T389} and Akt^{S473} in cells with wild-type levels of Rictor (+ vehicle; Figure 6, Supplementary Figure 2, available at *Carcinogenesis* Online), indicating activation of both mTORC1- and mTORC2-dependent pathways. Treatment with 4OHT to induce *rictor* recombination had little inhibitory effect on phosphorylation of the mTORC1 downstream effectors p70S6K1^{T389} and PRAS40^{T246} (Figure 6A). Total p70S6K1 and PRAS40 were also unchanged. The exception was at the 24-h time point, when significant cell toxicity was observed (data not shown). Interestingly, the phosphorylation of Akt^{T308} in response to UVB was increased slightly in the absence of Rictor (Figure 6A, Supplementary Figure 2A, available at *Carcinogenesis* Online).

In contrast to mTORC1 pathway intermediates, the robust UVB-dependent phosphorylation of AKT^{S473} observed in vehicle-treated cells was almost completely lost in cells with 4OHT-induced *rictor* recombination (Figure 6B, Supplementary Figure 2B, available at *Carcinogenesis* Online). This marked reduction in UVB-induced Akt^{S473} phosphorylation suggests that mTORC2 is the primary kinase that phosphorylates Akt in response to UVB, rather than the DNA-dependent protein kinase, a PIKK family kinase reported to phosphorylate Akt at Ser-473 in response to gamma irradiation (34). UVB-stimulated phosphorylation of forkhead box (FoxO) transcription factors 1/3a at Thr-24/32, which are targets of *p*-Akt^{S473} (1), was rapidly reduced in cells treated with 4OHT. This is particularly true for FoxO3a (top band in *p*-FoxO1/3a blot, Figure 6B), and was accompanied by a decrease in total FoxO3a with time after UVB (Figure 6B, Supplementary Figure 2B, available at *Carcinogenesis* Online). Since phosphorylation of FoxO1/3a by Akt is inhibitory to FoxO-dependent transcription of pro-apoptotic genes, these results suggest that, in Rictor-depleted cells, FoxO-dependent signaling is activated over several hours in response to UVB. Phosphorylation of PKCα/βII at Thr-638/641, whereas not significantly changed by UVB exposure, was decreased by about 40% in cells treated with 4OHT (Figure 6B, Supplementary Figure 2B, available at *Carcinogenesis* Online). This PKCα/βII phosphorylation site has been reported to require mTORC2 (5,6), and mTORC2 is also implicated in PKC stability (35). In agreement with this, total PKCα was also decreased in cells with Rictor disruption (Figure 6B, Supplementary Figure 2B, available at *Carcinogenesis* Online).

Discussion

In this study, we determined the role of the essential mTORC2 component Rictor during two-stage DMBA/TPA carcinogenesis in mouse skin. Using a Cre/LoxP approach to enable both spatial and temporal control of gene deletion, we found that absence of Rictor in the hair follicle and basal layer of the epidermis had no effect on normal epidermis stimulated to proliferate by multiple applications of TPA. In contrast, when *rictor* was ablated prior to initiation, mice were markedly more resistant to DMBA/TPA-induced tumor development than controls. Silencing of Rictor expression in tumor-bearing animals triggered regression of established tumors accompanied by increased levels of apoptosis without changes in proliferation. *In vitro* studies suggest the increased sensitivity to apoptosis in the absence of Rictor is mediated through mTORC2-dependent control of *p*-Akt^{Ser473} signaling without alterations in pathways controlled by mTORC1. These data provide strong evidence that mTORC2 is necessary for both skin tumor development and maintenance of established tumors.

Previous work has established that Rictor plays an essential role in the developing embryo (3), whereas conditional deletion of *rictor* in adipose tissue, liver and brain revealed the functional importance of mTORC2 in these organs (27,36,37). To investigate the contribution of mTORC2 to normal epidermal homeostasis and skin carcinogenesis, we used a model in which *rictor* recombination is driven by the Keratin 14 promoter in a 4OHT inducible manner, resulting in loss of *rictor* in the basal layer of the epidermis. We first showed that *rictor* deletion in adult epidermis caused no apparent defects in skin architecture and did not alter the proliferation response to multiple applications of

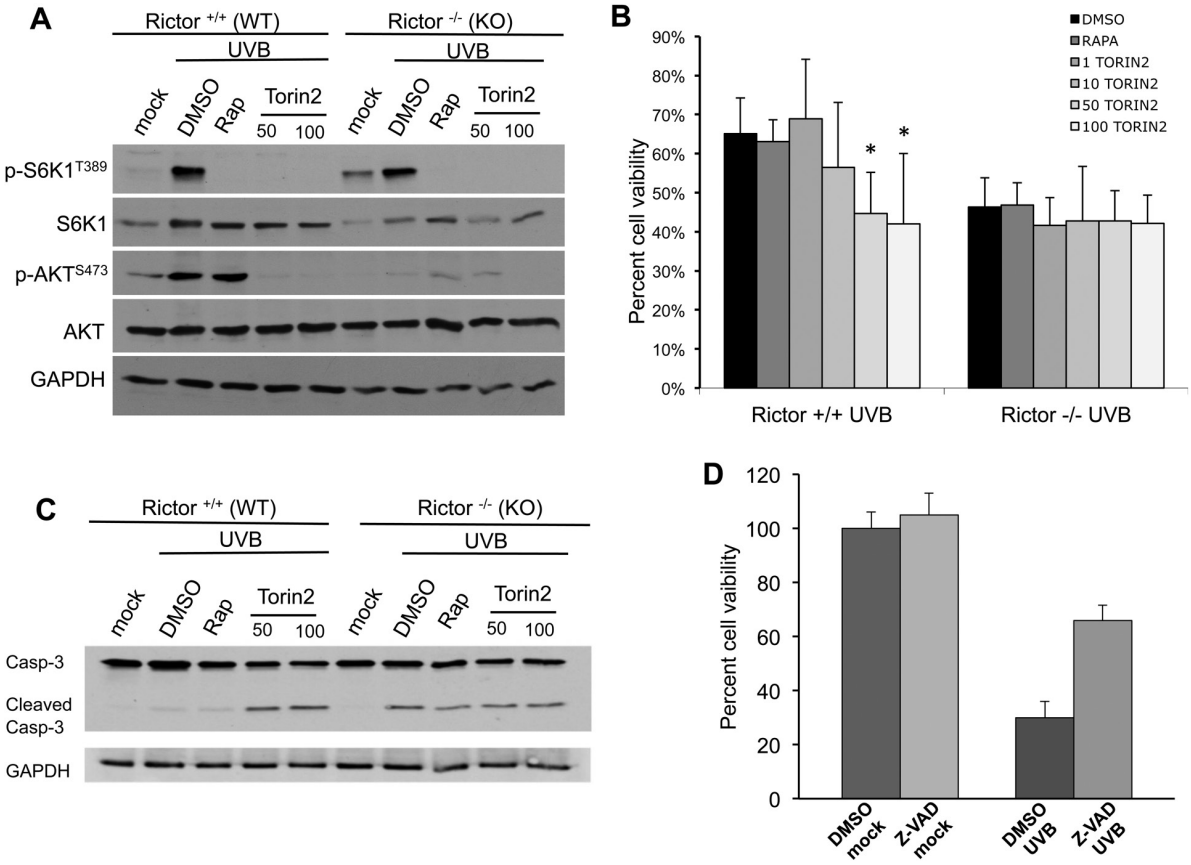

Figure 5. Effect of rapamycin or Torin-2 treatment of wild-type and Rictor-deficient cells on UVB-induced cell death. (**A–C**) Rictor wild-type (+/+) and knock-out (–/–) MEFs were treated with rapamycin (50 nM), various doses of Torin-2 (nM) or DMSO for 1 h prior to UVB (20 mJ/cm^2). (**A**) Whole cell lysates were harvested in RIPA buffer at 2 h post-UVB and subjected to immunoblot analysis of mTORC1 and mTORC2 activation markers. (**B**) MTS cell viability at 12 h post-UVB exposure showing % change in viability with UVB; $^*P < 0.05$. (**C**) Immunoblot analysis of CC3, at 12-h post-UVB. Data are representative of 2–3 independent experiments. (**D**) iRicKO cells were treated with either vehicle or with 4OHT for 3 days to induce *rictor* recombination, as described in the Materials and Methods. On day four, cells were pre-incubated with DMSO or 50 μM Z-VAD-fmk for 1 h, then exposed to 50 mJ/cm^2 UVB or mock-irradiated. Cells were harvested 24 h later and cell viability was measured by MTS assay. Data are representative of 2 independent experiments.

TPA, despite a dramatic reduction in epidermal *p*-Akt^{S473}. This is consistent with previous studies in *Drosophila*, where loss of Akt hydrophobic motif phosphorylation had little effect on normal tissue growth (38). Similarly, Rictor-dependent phosphorylation of Akt^{S473} was shown to be non-essential in mouse skeletal muscle and normal prostate epithelium (26,39). Akt is both upstream of mTORC1 and downstream of mTORC2, and dual phosphorylation of Akt at Ser473 by mTORC2 and Thr308 by PDK1, which is a component of the PI3-kinase signaling cascade, is required for complete activation (1). Because the absence of *p*-Akt^{S473} affects only a subset of Akt targets (40), our results suggest that normal epidermal proliferation is dependent on substrates of *p*-Akt^{T308}, and consequently requires mTORC1. Although signaling intermediates other than Akt are also involved in epidermal proliferation, our findings are in agreement with previous results showing that rapamycin potently inhibits TPA-induced epidermal hyperproliferation (24), and that overexpression of a constitutively activated form of Akt in the skin causes a hyperplastic epidermal phenotype (21).

Using a chemical carcinogenesis protocol, we went on to investigate the effect of *rictor* ablation on skin tumor development. Our previous studies suggest that mTORC2-dependent pathways control keratinocyte survival signaling in response to DNA damage (25). We therefore took advantage of the inducible nature of the K14-CreER^T transgene to direct *rictor* recombination prior to DMBA initiation. Rictor deficiency in the skin dramatically delayed tumor development compared with both control groups, and tumors from 4OHT-treated Cre-Rictor$^{L/L}$ mice averaged over 90% fewer in number and smaller in size. Thus, mTORC2 is necessary for skin tumor initiation, but not for keratinocyte proliferation. Our results fit with those demonstrating that mTORC2 is required for prostate tumor development in PTEN$^{-/-}$ mice (15,39), and also reinforce previous observations of aberrant Akt activation in mouse models of non-melanoma skin cancer (19,21). Taken together, these data support the hypothesis that mTORC2 is essential to maintain high Akt signaling in these tumor types. PCR analysis of tumors from Cre-Rictor$^{L/L}$ mice treated with 4OHT revealed the presence of the recombined *rictor* allele in 4 of 6 tumors (data not shown). However, this does not rule out the possibility that these tumors arose from initiated cells that escaped recombination.

An equally important and novel finding in our study is that disruption of *rictor* after tumors had formed not only prevented further growth, but also led to tumor regression. Furthermore, this regression occurs without changes in proliferation but with increased cleavage of caspase-3, consistent with increased apoptosis. These results suggest that mTORC2 plays a critical role in mediating keratinocyte survival pathways, and identify mTORC2

as a target for both prevention and treatment of non-melanoma skin cancer. Furthermore, since cutaneous squamous cell carcinoma often becomes resistant to standard cisplatin therapy (41), our clonogenic data support the study of TORC2 inhibitors as a therapeutic option in the setting of cisplatin resistance.

As an extension of our *in vivo* studies, we demonstrated that cells with loss of *rictor* are sensitized to caspase-dependent apoptosis in response to carcinogen exposure *in vitro*. Further, we observed reduced *p*-Akt^{Ser473} in *rictor*-deficient primary keratinocytes and MEFs. It is known that mTORC2 phosphorylation of Akt at Ser-473 promotes cell survival through a number of downstream effectors (2–6,42). Whereas dual phosphorylation of Akt at Thr-308 and Ser-473 is necessary for its full activation, Ser-473 phosphorylation alone is sufficient for Akt to inhibit FoxO1/3a transcription factors by phosphorylating multiple residues that cause sequestration of FoxO in the cytoplasm (40). When *p*-Akt^{S473} is inhibited, unphosphorylated FoxO translocates to the nucleus and activates transcription of apoptosis effectors such as FasL, TRAIL and the Bcl-2 homology domain (BH3)-only proteins (43,44). Our results show a selective reduction in *p*-Akt^{S473} without reduced *p*-Akt^{T308} in 4OHT-treated iRicKO cells exposed to UVB. FoxO1/3a phosphorylation at the Akt target site Thr-24/32 is decreased in these cells, consistent with FoxO1/3a activation when cells that lack Rictor are subjected to a carcinogenic stimulus.

Rictor has been reported to act independently of mTORC2 through functional interactions with a number of proteins. Protein complexes of Rictor with PKCζ, Myo1C, and inhibitor of nuclear factor κ-B kinase (IKK) are all associated with changes in actin cytoskeletal organization (45–47). The Rictor-Cullin 1

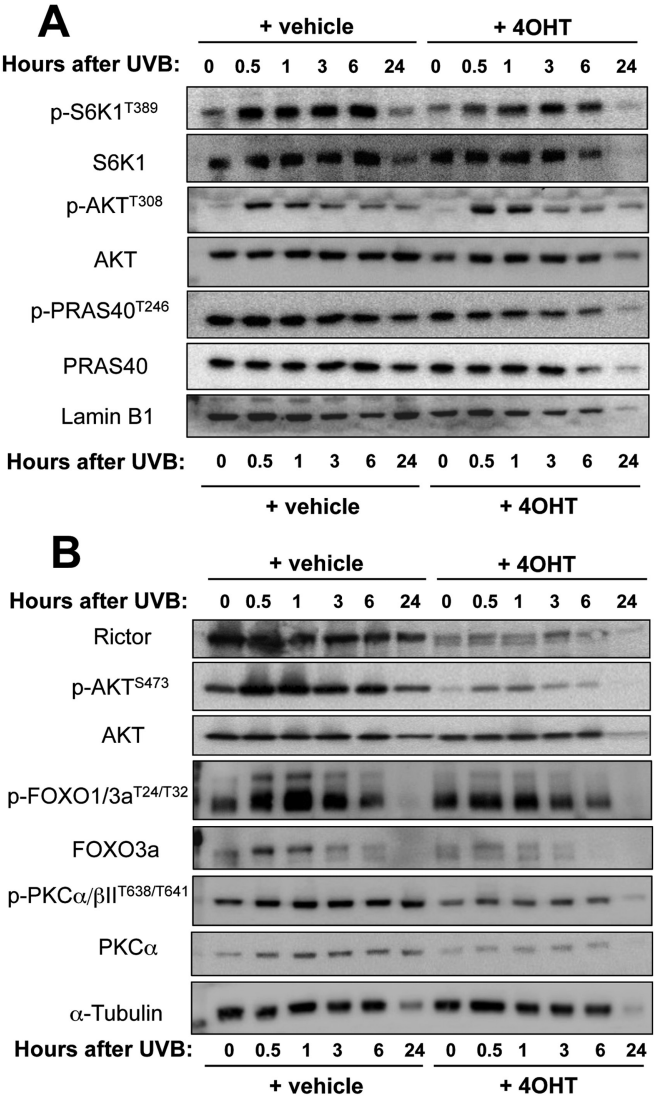

Figure 6. Biochemical analysis of mTORC1- and mTORC2-dependent signaling in response to UVB. iRicKO cells were treated with vehicle or with 4OHT for 3 days to induce *rictor* recombination. On day four, cells were exposed to 20 mJ/cm^2 UVB, and harvested in 1× sodium dodecyl sulfate sample buffer at the indicated time points for immunoblot analysis. For each protein analyzed, samples from both treatment groups are loaded onto the same gel to allow direct comparison of protein expression levels. (**A**) Expression of mTORC1 signaling intermediates over a time course from T = 0 to T = 24 h after UVB exposure. (**B**) Expression of mTORC2 signaling intermediates over the same time course. Quantitation of blots is shown in Supplementary Figures 1A and B is available at *Carcinogenesis* Online. Phosphorylated proteins were normalized to their corresponding total protein on the same gel and other proteins were normalized to either Lamin B1 or Tubulin on the same gel, as described in the legend for Supplementary Figure 2, available at *Carcinogenesis* Online. One Lamin B1 blot and one Tubulin blot are shown for reference. Results are representative of 2–3 independent experiments.

complex acts as an E3 ubiquitin ligase to control degradation of the serum and glucocorticoid-inducible kinase (48). Serum and glucocorticoid-inducible kinase, like Akt, is an AGC kinase that can phosphorylate FoxO1/3a (49). However, unlike Akt, which is negatively regulated by loss of Rictor, serum and glucocorticoid-inducible kinase is induced in Rictor$^{-/-}$ MEFs as a result of increased protein stability (48). Since we see reduced FoxO phosphorylation in UVB-treated iRicKO cells, this suggests that Akt signaling is dominant in our system. It has also been found that a complex between Rictor and integrin-linked kinase can regulate Akt^{S473} phosphorylation and cell survival in the absence of mTOR in a subset of human breast cancer cell lines (50). Although an mTORC2-independent function of Rictor in cell survival signaling cannot be completely ruled out from our studies, we show that the mTOR kinase inhibitor Torin-2 sensitizes wild-type but not Rictor$^{-/-}$ MEFs to UVB-induced apoptosis, supporting the hypothesis that mTORC2 initiates pro-survival signaling in response to carcinogen treatment by activation of Akt-dependent pathways.

In summary, these studies show for the first time that, while dispensable for normal keratinocyte proliferation, mTORC2 is essential for both skin tumor development and maintenance of established tumors. They further suggest that mTORC2 controls pro-survival pathways both *in vitro* and in tumors. Although the development of mTORC2-specific inhibitors has been elusive, our results support the idea that activated Akt signaling will render specific tumor types more responsive to therapy targeting the mTOR pathway.

Supplementary Material

Supplementary Table 1, Figures 1 and 2 and scans of original gels used for Western analyses can be found at http://carcin.oxfordjournals.org/

Funding

National Institutes of Health (ES019242 to L.M.S.); T.D.C. is the recipient of an MD/PhD pre-doctoral fellowship (F30 ES019809).

Acknowledgements

We thank Suzanne Sass-Kuhn for excellent technical assistance, the technicians of the Penn State University College of Medicine Department of Comparative Medicine for expert animal care, and the Penn State University College of Medicine Macromolecular Synthesis and Sequencing Cores.
Conflict of Interest Statement: None declared.

References

1. Zoncu, R. et al. (2011) mTOR: from growth signal integration to cancer, diabetes and ageing. Nat. Rev. Mol. Cell Biol., 12, 21–35.
2. Hresko, R.C. et al. (2005) mTOR.RICTOR is the Ser473 kinase for Akt/protein kinase B in 3T3-L1 adipocytes. J. Biol. Chem., 280, 40406–40416.
3. Guertin, D.A. et al. (2006) Ablation in mice of the mTORC components raptor, rictor, or mLST8 reveals that mTORC2 is required for signaling to Akt-FOXO and PKCalpha, but not S6K1. Dev. Cell, 11, 859–871.
4. Sarbassov, D.D. et al. (2004) Rictor, a novel binding partner of mTOR, defines a rapamycin-insensitive and raptor-independent pathway that regulates the cytoskeleton. Curr. Biol., 14, 1296–1302.
5. Facchinetti, V. et al. (2008) The mammalian target of rapamycin complex 2 controls folding and stability of Akt and protein kinase C. EMBO J., 27, 1932–1943.
6. Ikenoue, T. et al. (2008) Essential function of TORC2 in PKC and Akt turn motif phosphorylation, maturation and signalling. EMBO J., 27, 1919–1931.
7. Jacinto, E. et al. (2004) Mammalian TOR complex 2 controls the actin cytoskeleton and is rapamycin insensitive. Nat. Cell Biol., 6, 1122–1128.
8. Masri, J. et al. (2007) mTORC2 activity is elevated in gliomas and promotes growth and cell motility via overexpression of rictor. Cancer Res., 67, 11712–11720.
9. Hernández-Negrete, I. et al. (2007) P-Rex1 links mammalian target of rapamycin signaling to Rac activation and cell migration. J. Biol. Chem., 282, 23708–23715.
10. Kim, E.K. et al. (2011) Selective activation of Akt1 by mammalian target of rapamycin complex 2 regulates cancer cell migration, invasion, and metastasis. Oncogene, 30, 2954–2963.
11. Gulhati, P. et al. (2011) mTORC1 and mTORC2 regulate EMT, motility, and metastasis of colorectal cancer via RhoA and Rac1 signaling pathways. Cancer Res., 71, 3246–3256.
12. Fruman, D.A. et al. (2014) PI3K and cancer: lessons, challenges and opportunities. Nat. Rev. Drug Discov., 13, 140–156.
13. Sun, S.Y. et al. (2005) Activation of Akt and eIF4E survival pathways by rapamycin-mediated mammalian target of rapamycin inhibition. Cancer Res., 65, 7052–7058.
14. O'Reilly, K.E. et al. (2006) mTOR inhibition induces upstream receptor tyrosine kinase signaling and activates Akt. Cancer Res., 66, 1500–1508.
15. Nardella, C. et al. (2009) Differential requirement of mTOR in postmitotic tissues and tumorigenesis. Sci. Signal., 2, 1–11.
16. Im-aram, A. et al. (2013) The mTORC2 component rictor contributes to cisplatin resistance in human ovarian cancer cells. PLoS One, 8, e75455.
17. Chen, S.J. et al. (2009) Activation of the mammalian target of rapamycin signalling pathway in epidermal tumours and its correlation with cyclin-dependent kinase 2. Br. J. Dermatol., 160, 442–445.
18. Einspahr, J.G. et al. (2012) Functional protein pathway activation mapping of the progression of normal skin to squamous cell carcinoma. Cancer Prev. Res. (Phila)., 5, 403–413.
19. Suzuki, A. et al. (2003) Keratinocyte-specific Pten deficiency results in epidermal hyperplasia, accelerated hair follicle morphogenesis and tumor formation. Cancer Res., 63, 674–681.
20. Segrelles, C. et al. (2002) Functional roles of Akt signaling in mouse skin tumorigenesis. Oncogene, 21, 53–64.
21. Segrelles, C. et al. (2007) Deregulated activity of Akt in epithelial basal cells induces spontaneous tumors and heightened sensitivity to skin carcinogenesis. Cancer Res., 67, 10879–10888.
22. Back, J.H. et al. (2012) Resveratrol-mediated downregulation of Rictor attenuates autophagic process and suppresses UV-induced skin carcinogenesis. Photochem. Photobiol., 88, 1165–1172.
23. Perez-Losada, J. et al. (2003) Stem-cell hierarchy in skin cancer. Nat. Rev. Cancer, 3, 434–443.
24. Checkley, L.A. et al. (2011) Rapamycin is a potent inhibitor of skin tumor promotion by 12-O-tetradecanoylphorbol-13-acetate. Cancer Prev. Res. (Phila)., 4, 1011–1020.
25. Carr, T.D. et al. (2012) Inhibition of mTOR suppresses UVB-induced keratinocyte proliferation and survival. Cancer Prev. Res. (Phila)., 5, 1394–1404.
26. Bentzinger, C.F. et al. (2008) Skeletal muscle-specific ablation of raptor, but not of rictor, causes metabolic changes and results in muscle dystrophy. Cell Metab., 8, 411–424.
27. Cybulski, N. et al. (2009) mTOR complex 2 in adipose tissue negatively controls whole-body growth. Proc. Natl. Acad. Sci. U. S. A., 106, 9902–9907.
28. Vasioukhin, V. et al. (1999) The magical touch: genome targeting in epidermal stem cells induced by tamoxifen application to mouse skin. Proc. Natl. Acad. Sci. U. S. A., 96, 8551–8556.
29. Cybulski, N. et al. (2012) Inducible raptor and rictor knockout mouse embryonic fibroblasts. Methods Mol. Biol., 821, 267–278.
30. Shiota, C. et al. (2006) Multiallelic disruption of the rictor gene in mice reveals that mTOR complex 2 is essential for fetal growth and viability. Dev. Cell, 11, 583–589.
31. Sarbassov, D.D. et al. (2006) Prolonged rapamycin treatment inhibits mTORC2 assembly and Akt/PKB. Mol. Cell, 22, 159–168.
32. Zeng, Z. et al. (2007) Rapamycin derivatives reduce mTORC2 signaling and inhibit AKT activation in AML. Blood, 109, 3509–3512.
33. Amornphimoltham, P. et al. (2008) Inhibition of Mammalian target of rapamycin by rapamycin causes the regression of carcinogen-induced skin tumor lesions. Clin. Cancer Res., 14, 8094–8101.

34. Surucu, B. et al. (2008) *In vivo* analysis of protein kinase B (PKB)/Akt regulation in DNA-PKcs-null mice reveals a role for PKB/Akt in DNA damage response and tumorigenesis. J. Biol. Chem., 283, 30025–30033.
35. Oh, W.J. et al. (2011) mTOR complex 2 signaling and functions. Cell Cycle, 10, 2305–2316.
36. Hagiwara, A. et al. (2012) Hepatic mTORC2 activates glycolysis and lipogenesis through Akt, glucokinase, and SREBP1c. Cell Metab., 15, 725–738.
37. Thomanetz, V. et al. (2013) Ablation of the mTORC2 component rictor in brain or Purkinje cells affects size and neuron morphology. J. Cell Biol., 201, 293–308.
38. Hietakangas, V. et al. (2007) Re-evaluating AKT regulation: role of TOR complex 2 in tissue growth. Genes Dev., 21, 632–637.
39. Guertin, D.A. et al. (2009) mTOR complex 2 is required for the development of prostate cancer induced by Pten loss in mice. Cancer Cell, 15, 148–159.
40. Jacinto, E. et al. (2006) SIN1/MIP1 maintains rictor-mTOR complex integrity and regulates Akt phosphorylation and substrate specificity. Cell, 127, 125–137.
41. Neville, J.A. et al. (2007) Management of nonmelanoma skin cancer in 2007. Nat. Clin. Pract. Oncol., 4, 462–469.
42. Sarbassov, D.D. et al. (2005) Phosphorylation and regulation of Akt/PKB by the rictor-mTOR complex. Science, 307, 1098–1101.
43. Greer, E.L. et al. (2005) FOXO transcription factors at the interface between longevity and tumor suppression. Oncogene, 24, 7410–7425.
44. Hers, I. et al. (2011) Akt signalling in health and disease. Cell. Signal., 23, 1515–1527.
45. Zhang, F. et al. (2010) mTOR complex component Rictor interacts with PKCzeta and regulates cancer cell metastasis. Cancer Res., 70, 9360–9370.
46. Hagan, G.N. et al. (2008) A Rictor-Myo1c complex participates in dynamic cortical actin events in 3T3-L1 adipocytes. Mol. Cell. Biol., 28, 4215–4226.
47. Xu, Y. et al. (2013) IKK interacts with rictor and regulates mTORC2. Cell. Signal., 25, 2239–2245.
48. Gao, D. et al. (2010) Rictor forms a complex with Cullin-1 to promote SGK1 ubiquitination and destruction. Mol. Cell, 39, 797–808.
49. Brunet, A. et al. (2001) Protein kinase SGK mediates survival signals by phosphorylating the forkhead transcription factor FKHRL1 (FOXO3a). Mol. Cell. Biol., 21, 952–965.
50. McDonald, P.C. et al. (2008) Rictor and integrin-linked kinase interact and regulate Akt phosphorylation and cancer cell survival. Cancer Res., 68, 1618–1624.